Preferential Location of Ge in the Double Four-Membered Ring Units of ITQ-7 Zeolite

Teresa Blasco, Avelino Corma,* Mª José Díaz-Cabañas, Fernando Rey, José A. Vidal-Moya, and Claudio M. Zicovich-Wilson

Instituto de Tecnología Química, UPV-CSIC, Universidad Politécnica de Valencia, Avda. de los Naranjos s/n, 46022 Valencia, Spain

Received: August 27, 2001; In Final Form: November 25, 2001

ITQ-7 is a tri-dimensional twelve-membered ring zeolite which presents double four-membered ring units (D4MR) in its structure. On the basis of theoretical ab initio calculations, which indicate that isomorphic substitution of Ge for Si atoms in the double four-membered ring units stabilizes such small cages, we have carried out the synthesis of ITQ-7 in the presence of Ge. It is found that the incorporation of Ge reduces the crystallization time from 7 days to less than 12 h, while a detailed analysis of the ^{19}F and ^{29}Si MAS NMR leads to the conclusion that Ge selectively occupies positions at the D4MR. An hypothesis has been introduced which assumes that the increase in the crystallization rate is due to the preferential occupancy of D4MR sites by Ge, and this allows relaxation of the constrained T−O−T bonds of these small D4MR cages.

Introduction

The widespread interest of researchers in zeolites is due not only to their use in technologically important processes such as adsorption, separation, and catalysis, but also to the fact that they offer to scientists the opportunity to rationalize their adsorption and catalytic findings from the structural and physicochemical characteristics of these materials. Thus, the ultimate goal of researchers working in the field of zeolites would be to design and to carry out the tailor-made synthesis of a zeolite structure with the most adequate pore topology for a particular application. Unfortunately, the present knowledge is not yet at the point that allows the tailor-made synthesis of zeolites. However, important advances have been made through the rational design of structure-directing (SDA) organic molecules, which have a strong influence on the final zeolite structures.[1−4] In that way, the control of parameters such as rigidity, polarity, and spatial structure of the SDA have been found to be of paramount importance for synthesizing new zeolite structures.[1]

Besides the nature of the SDA it appears quite logical to assume that the nature of the framework atoms, which allows T−O−T bonds with different distances and angles to be formed, can influence the relative stability of different secondary building units (SBU), directing or facilitating the synthesis toward one particular zeolite structure by increasing its rate of nucleation. In this sense, little differences in energy are found in Si−O−Si angles between 140° and 180°, allowing the formation of different silicates having Si−O−Si linkages in that range.[5] However, for angles below 140° a high increase of energy was found,[5] with the corresponding decrease in stability of the zeolite structure containing those low angles. To overcome this limitation, the incorporation of other elements different than silicon into the framework, which decrease the energy of the Si−O−M bond by forming angles lower than 140°, has been attempted. For example, Zn strongly directs to the formation of three-membered rings leading to the crystallization of VPI-8 by using a series of organic structure-directing agents, inhibiting therefore the formation of other high-silica zeolites.[6] These results were taken as a proof that the presence of Zn is a more important structure-directing parameter than the nature of the organic SDA used for the synthesis of VPI-8.

Recently, a new pure silica zeolite named ITQ-7 (that stands for Instituto de Tecnología Química-seven) with a tridimensional system of 12 MR pore channels structure (IZA code: ISV) has been synthesized.[7] This material contains two non-equivalent double four-membered ring (D4MR) cages, and it appears that the presence of the very small D4MR cavities, with the corresponding stressed T−O−T bonds, decreases the stability of the ITQ-7 structure[8] and precludes an easy isomorphic substitution of other heteroatoms different than silicon. Indeed, attempts of direct incorporation of Al^{III} into the ITQ-7 structure were unsuccessful, and also Ti was only incorporated at the level of traces (Si/Ti > 100). When higher loading of Ti was introduced into the synthesis gel, the crystallization of ITQ-7 stops before reaching a fully-developed crystal structure.

At this point, we thought that the geometric constraints in the D4MR cages could be diminished by Ge incorporation into D4MR structural sites. Indeed, while the isomorphous substitution of Si by tetravalent Ge retains the neutral charged zeolite lattice, it will increase the average T−O distance and decrease the T−O−T angle, relaxing the structure and making it more stable. In fact, O'Keeffe and Yaghi have proposed that pure Ge zeolitic materials can be synthesized only if the structures contains T−O−T angles close to 130°, which is the preferred for Ge−O bonds.[9] This has been the case of ASU-9, with a structure similar to the siliceous octadecasil (AST), and ASU-7 materials, which does not possess its siliceous counterpart.[10] The structure-stabilizing effect related to the presence of framework Ge atoms in quite constrained zeolites has been also pointed out in a recent theoretical study on several Ti-zeolites where Si atoms have been isomorphically substituted by Ge.[11] In that case it has been observed that the formation of tetrahedral Ti centers is favored in such materials owing to the additional structural flexibility given by the framework Ge cations. Furthermore, theoretical calculations reported here using a

* Author to whom correspondence should be addressed. Tel: 34(96)3877800. Fax: 34(96)3877809. E-mail: acorma@itq.upv.es.

10.1021/jp013302b CCC: $22.00
Published on Web 02/14/2002

cluster constituted by a D4MR unit, confirmed the increase in stability of the Ge-containing structure with respect to analogous pure siliceous clusters and encouraged us to also attack the synthesis of Ge-substituted ITQ-7 materials.

In this work we show that the presence of Ge into the synthesis gel strongly increases the rate of crystallization of ITQ-7 materials and, even more relevant, we show that Ge is preferentially incorporated into the D4MR units, together with the F^- ions, these two factors being determinant for the stabilization of the D4MR containing structure.

Experimental Section

Materials. Ge-ITQ-7 samples were prepared under hydrothermal conditions from a gel having the following molar composition:

$$x\mathrm{GeO_2}: (1-x)\mathrm{SiO_2}:0.50\mathrm{C_{14}H_{26}NOH}:0.50\mathrm{HF}:3\mathrm{H_2O}$$

where x was varied between 0 and 0.5. $C_{14}H_{26}NOH$ was 1,3,3-trimethyl-6-azonium tricyclo[3.2.1.$4^{6,6}$]dodecane hydroxide used as the structure-directing agent. The gels were prepared by dissolving germanium oxide in the 1,3,3-trimethyl-6-azonium tricyclo[3.2.1.$4^{6,6}$]dodecane hydroxide solution. Then, tetraethyl orthosilicate was hydrolyzed in that solution and the mixture was mechanically stirred at room temperature until complete elimination of the ethanol formed and the amount of water required to reach the final composition. Finally, HF was added and the mixture was homogenized. The resulting reaction mixture was autoclaved at 150 °C under static conditions in Teflon-lined stainless steel autoclaves. Samples were taken at different times in order to build the crystallization curves for each gel composition. The solids were recovered by filtration, washed with distilled water, and dried at 100 °C.

Physicochemical Techniques. Phase purity and crystallinity were determined by X-ray powder diffraction data, recorded in a Philips X′Pert MPD diffractometer equipped with a PW3050 goniometer (Cu Kα radiation, graphite monochromator) provided with variable divergence and anti-scatter slits and working in the fixed irradiated area mode. The XRD peak positions were extracted by carrying out the full-fit profile using the Profit v1.0c program. Then, unit cell dimensions were calculated from these reflections using the X′Pert Plus v1.0 (program for crystallography and Rietveld analysis) program. The Ge content was analyzed with a Varian SpectraAA-10Plus and the standard deviations obtained for samples with a well-known Ge content were below 5%. The chemical analyses agree fairly well with those obtained by using EDAX. N, C, and H contents were determined with a Carlo Erba 1106 elemental organic analyzer. Fluoride was determined[12] using an ion-selective electrode connected to a Mettler Toledo 355 ion analyzer. The crystal size and morphology were monitored by scanning electron microscopy (SEM) using a JEOL JSM-6300 microscope. Finally, the IR spectra in the region of framework vibrations were recorded in a Nicolet 710 FTIR spectrometer using the KBr pellet technique. N_2 isotherms were obtained in a ASAP 2010 Micromeritics apparatus.

^{29}Si and ^{19}F solid-state NMR spectra were recorded under magic angle spinning (MAS) at ambient temperature with a Varian VXR-S 400 WB spectrometer at 79.5 and 376.3 MHz, respectively. The ^{29}Si and ^{19}F chemical shifts were referred to TMS and $CFCl_3$, respectively. An RT CP/MAS Varian probe with zirconia rotors (7 mm in diameter) was used for ^{29}Si. ^{19}F and ^{19}F to ^{29}Si cross polarization (CP) experiments were carried out with a Doty XC4 probe using silicon nitride and zirconia rotors, respectively, of 4 mm outer diameter. The ^{29}Si Bloch decay (BD) spectra were acquired using pulses of 4 μs to flip the magnetization an angle of $^3/_4\pi$ radians, and a recycle delay of 240 s. The inversion recovery pulse sequence was used to measure the longitudinal relaxation time of ^{19}F in these samples, which gave a value of $T_1 \simeq 17$ s. The ^{19}F to ^{29}Si cross polarization conditions were optimized using a sample of Na_2SiF_6, while the best contact time was estimated on a real sample. The ^{19}F $\pi/2$ pulse length was 5 μs, and the contact time 5 ms. A recycle delay of 80 s was used to ensure the complete recovery of the ^{19}F magnetization. A similar delay was used to record the ^{19}F spectra, with pulses of 5 μs corresponding to a magnetization flip angle of $\pi/2$, and spinning rates in the range 15−17 kHz. The ^{19}F background signal coming from the stator was subtracted from the spectra of the samples.

Computational Details. Calculations have been performed on model clusters constituted by a double four-membered ring unit (D4MR) with OH groups saturating the linkages with the rest of the framework. The models considered differ in the number of Si and Ge atoms occupying tetrahedral positions. Five models have been considered, namely: M_0, M_1, M_2, $M_{2'}$, and M_3. The generic chemical formula of model M_n is $Si_{8-n}Ge_nO_{20}H_8$. Concerning M_2 and $M_{2'}$, they differ in the relative position of the two Ge atoms; in the former, Ge atoms are located at opposite sites along the longest diagonal of the D4MR cage, while in the latter they are occupying consecutive corners of the D4MR unit.

The stability of the different D4MR units has been estimated with respect to two references consisting of (1) molecular species expected in aqueous media during synthesis: $Si(OH)_4$ and $Ge(OH)_4(H_2O)_2$, and (2) solid species SiO_2 and GeO_2 in the form of α-quartz and rutile type crystalline structures, respectively.

Calculations have been performed at the Hartree−Fock level of theory using the standard quantum chemistry codes Gaussian 94[13] and CRYSTAL 98[14] for molecular and crystalline systems, respectively. To make possible the comparison between periodic and molecular systems, a basis set suitable for both types of calculations has been employed. The set consists of the following Contracted Gaussian Type Orbitals: 6-31G(d), 6-21G(d), 31G and (26s, 17p, 7d)/[5s, 4p, 1d] for O, Si, H, and Ge, respectively. Details of the basis set can be obtained from refs 11 and 15.

Cluster models and reference molecules have been optimized using gradient techniques and redundant internal coordinates. Optimization of models M_n has been carried out by keeping fixed the angle TOH (120°) and constraining the rotation of the terminal OH groups around the TO bond. Indeed, the modes frozen are no longer relevant for the present study as they do not represent any structural feature of the actual zeolitic framework. In addition the related force constants are quite small which would result in unnecessarily large optimizations. The rest of the geometrical parameters have been fully relaxed. Concerning the reference molecules, $Si(OH)_4$ and $Ge(OH)_4(H_2O)_2$, they have been fully optimized. The geometries of the periodic SiO_2 and GeO_2 are also optimal at the present calculation level and have been obtained from ref 11.

Results and Discussion

Theoretical Results. The hypothesis that the substitution of Ge for Si at the tetrahedral (T) sites located at the double D4MRs increases the stability of the cage was first studied by theoretical calculations.

Prior to a discussion of the relative stability of the proposed Ge-containing D4MR models, let us consider their optimized geometries summarized in Table 1, in particular the average

TABLE 1: Relevant Geometrical Features of the Optimized Ge-Containing D4MR Models (distances in Å, angles in °); av = average, and dev = standard deviation

parameter	M_0	M_1	M_2	$M_{2'}$	M_3
av R(GeO)	-	1.719	1.719	1.721	1.721
av R (SiO)	1.615	1.615	1.615	1.615	1.616
av A (TOT)	149	148	148	148	146
dvA (TOT)	6	7	8	6	10
dv A (OTO)	1.2	1.2	1.2	1.5	1.7

TABLE 2: Relative Stability (kcal mol^{-1}) of the Ge-Containing D4MR Models

	M_0	M_1	M_2	$M_{2'}$	M_3
ΔE_{aq}	−32.1	−35.3	−38.6	−38.3	−42.3
ΔE_{sld}	31.5	27.6	23.7	24.0	19.3

GeO and SiO bond distances (av *R*(GeO) and av *R*(SiO), respectively), the average TOT angles (av *A*(TOT)) and the standard deviation of both TOT and OTO angles (dv *A*(TOT) and dv *A*(OTO), respectively). The average values of the optimized distances and angles of models M_n are quite similar, indicating that substitution has no strong additional internal constraints in the unit. Concerning the deviations of the TOT and OTO angles, it arises that the maximum distortion of the TO_4 tetrahedra and dispersion of the TOT angle occurs in models $M_{2'}$ and M_3. This is probably because of the occurrence of neighboring Ge atoms in both cases. The presence of two shared GeO_4 units in the D4MR model generates a distortion larger than that occurred when they are separated by SiO_4 units.

The relative stability of the proposed models has been calculated as the energetic balance of two different hypothetical reactions of formation of D4MRs with a composition $Si_{8-n}Ge_nO_{20}H_8$:

$$(8-n)Si(OH)_4 + nGe(OH)_4(H_2O)_2 \rightarrow Si_{8-n}Ge_nO_{20}H_8 + (12+2n)H_2O \quad (1)$$

$$(8-n)SiO_2(s) + nGeO_2(s) + 4H_2O \rightarrow Si_{8-n}Ge_nO_{20}H_8 \quad (2)$$

Equation 1 can be viewed as the formation reaction of D4MR units M_n in aqueous media. In this process, the stabilization due to solvation effects was not introduced in the calculation. On the other hand, eq 2 represents the formation of a D4MR unit of the same composition starting from solid SiO_2 and GeO_2. The reaction energy values in eqs 1 and 2 (ΔE_{aq} and ΔE_{sld}, respectively) for the five models considered are listed in Table 2. Interestingly, SiO_2 or GeO_2 can be considered as competitive products in the formation of the D4MR unit.

The energetic balances of reactions 1 and 2 indicate that the relative stability of the D4MR unit increases as increasing the Ge content irrespective of the relative positions of the Ge atoms. This is valid when considering both the hydrated molecules (ΔE_{aq}) and the solid SiO_2 and GeO_2 (ΔE_{sld}) as reference systems. From the present results, it turns out that the dependence of the reaction energies, and therefore of the relative stability, on the number of Ge atoms is almost linear with a slope of −3.4 and −4.1 kcal mol^{-1} for reactions 1 and 2, respectively.

Synthesis and XRD Characterization of the Samples. Theoretical calculations indicate that the incorporation of Ge can stabilize the D4MR units, which could also have a positive influence on the crystallization of ITQ-7. For this reason, we proceeded to the synthesis of ITQ-7 in the presence of Ge.

The results presented in Figure 1 show that the addition of germanium to the synthesis mixture up to a Si/Ge ratio (both in the gel and the solid) of 5 strongly reduces the crystallization time of ITQ-7 materials from ∼7 days to less than 12 h. For higher Ge contents, the crystallization rate decreases, but is still faster than that for the pure silica ITQ-7 zeolite.

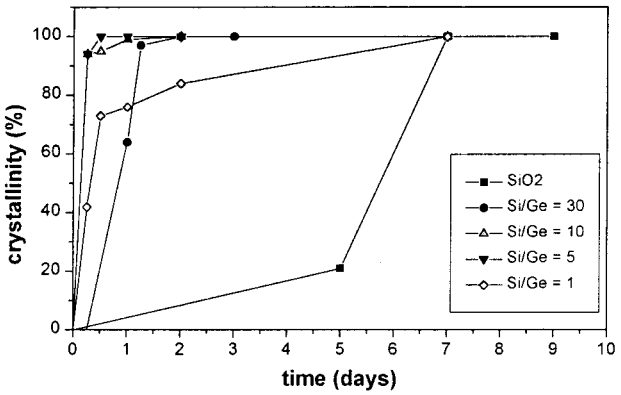

Figure 1. Crystallization curves of ITQ-7 materials with different Ge content.

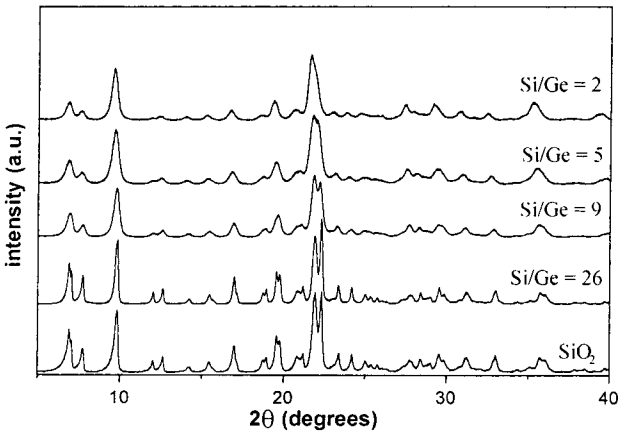

Figure 2. X-ray diffraction patterns of as-made Ge-ITQ-7 samples compared to that of pure silica.

The XRD patterns of siliceous and representative Ge-containing ITQ-7 samples are shown in Figure 2. The solids are fully crystallized and present all the characteristic reflections of ITQ-7 structure, while no amorphous material is detected. However, the reflections of the XRD patterns of Ge-ITQ-7 samples are broader than those observed for the siliceous ITQ-7, which could be attributed to their much smaller crystal size. In Figure 3, it can be clearly seen that Ge-ITQ-7 materials show a crystal size smaller than 0.1 μm, while the pure silica ITQ-7 presents a broad crystal size distribution between 1 and 10 μm. In fact, the simulated XRD patterns of ITQ-7 samples with different sizes (calculated using the Cerius[2] software from Molecular Simulation Inc.) indicate that the observed broadening of the XRD peaks would be consistent with Ge-ITQ-7 crystallites with average diameter below 100 nm. The high crystallinity of the Ge-containing samples has been further proved by comparing the micropore volume determined from the N_2 isotherm of the Ge-ITQ-7 samples (0.24 cm^3 g^{-1} for the sample having a Si/Ge ratio of 10) with that obtained for the purely siliceous material (0.25 cm^3 g^{-1})[7]. The large N_2 uptake observed at relatively high P/P_0 in the adsorption isotherms (Figure 4) confirms that these Ge-containing ITQ-7 possess a very small crystal size, this being responsible for the large surface area observed on Ge-ITQ-7 (651 m^2 g^{-1}) compared to the siliceous ITQ-7 material (543 m^2 g^{-1}). Then, textural properties further support the high crystallinity of the Ge-containing samples.

The chemical composition of the as-synthesized ITQ-7 samples (Table 3) indicates that the C/N ratio is close to that

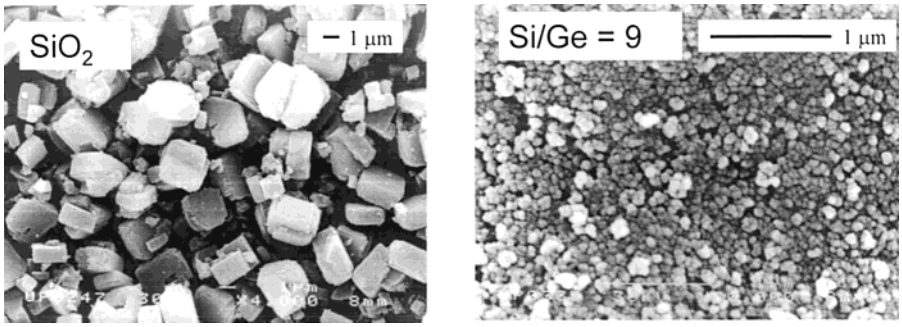

Figure 3. Scanning electron micrographs of pure silica ITQ-7 (left) and Ge-ITQ-7 (right).

TABLE 3: Chemical Composition of Ge-Containing ITQ-7 Samples

sample	Si/Ge (gel)	Si/Ge (sol)	yield (%) $g_{sol}/g_{SiO_2+GeO_2}$	% analyzed N	C	H	F	Ge	Rest TG	C/N	F/N	SDA/u.c.	F/u.c.
Si-ITQ-7	∞	∞	111.3	1.18	14.25	2.27	1.61	-	79.24	14.1	1.01	4.09	4.10
26Ge-ITQ-7	30	26	91.5	1.15	14.03	2.38	1.60	3.49	80.30	14.2	1.03	4.04	4.14
9Ge−ITQ-7	10	9	103.4	1.10	13.08	2.17	1.62	9.05	80.67	13.9	1.09	4.02	4.37
5Ge-ITQ-7	5	5	92.3	1.16	14.15	2.20	1.75	14.13	81.47	14.2	1.11	4.39	4.89
2Ge-ITQ-7	1	2.3	53.1	1.23	15.22	2.33	1.54	23.87	77.86	14.4	0.92	5.32	4.89

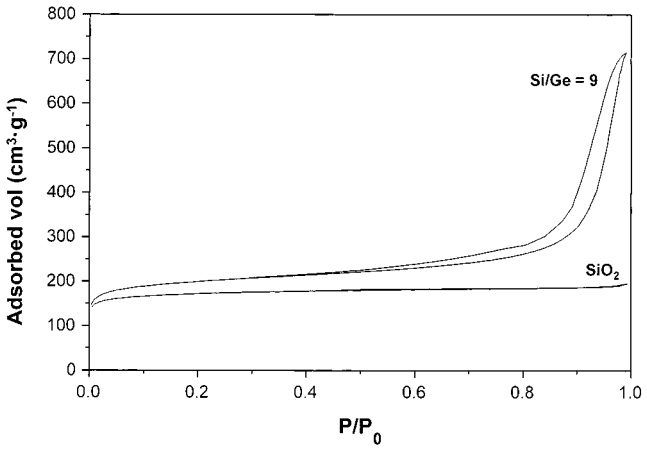

Figure 4. N_2 isotherms of the pure silica ITQ-7 and 9Ge-ITQ-7 sample.

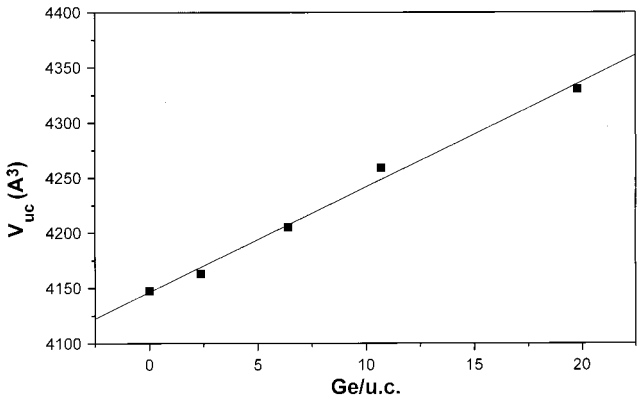

Figure 5. Unit cell volume toward Ge content in ITQ-7 samples.

of the organic SDA, suggesting that this remains intact inside the zeolite pores. Also, the F/N ratio close to 1 indicates that F^- anions are compensating the charge introduced by tetraalkylammonium cations, similarly to that observed in most materials synthesized in fluoride media.[16−18] It is remarkable that the amount of the SDA present in samples with Si/Ge ≥ 10 is similar to that of the pure silica ITQ-7. However, for the samples with higher Ge content (Si/Ge = 2 and 5) a small excess of SDA and fluoride ions has been found that could be located at the external surface of the very small zeolite crystallites formed.

Evidence of the Ge incorporation into framework positions of the ITQ-7 structure is obtained from the continuous shift of the characteristic XRD reflections to lower 2θ values (i.e., higher d-spaces) as the Ge content increases. Indeed, when the unit cell volumes are calculated from the XRD patterns of the Ge-containing ITQ-7 samples, a nearly linear correlation between the Ge content and the unit cell volume (Figure 5) is observed. Moreover, a slightly larger increase of the parameter *c* vs *a* was observed, indicating that there is a certain anisotropy in the Ge incorporation into the ITQ-7 framework.

IR Spectroscopy of Ge-ITQ-7. The IR spectra of Ge-ITQ-7 samples are presented in Figure 6. The vibration band of octahedrally coordinated GeO_6 which appears at 720 cm^{-1} [19] is not observed, suggesting that extraframework Ge species are not present in the crystalline samples.

The absorption bands at 1050, 1100, and 1225 cm^{-1} in the pure silica ITQ-7 can be assigned to asymmetric T−O−T (Si−O−Si) stretching vibrations. In Ge-containing ITQ-7, the intensity ratio of the 1100 to 1050 cm^{-1} bands increases, and a new band at ∼1000 cm^{-1} grows with the Ge content. The band at ∼1000 cm^{-1} can be assigned to asymmetric T−O−T stretching vibration of Si−O−Ge groups in the framework, in analogy to the changes occurring in the spectra of SiO_2-GeO_2 glasses when increasing Ge content from 0 to 16 GeO_2 wt %.[19] IR bands at 890 and 570 cm^{-1} appear in the Ge-ITQ-7, being more intense for the sample with the lowest Si/Ge ratio. These bands are present in the pure germanium form of octadecasil,[20] and can be assigned to the symmetric and asymmetric T−O−T vibration bands of Ge−O−Ge groups, respectively.[21]

In summary, the IR bands appearing as a consequence of the Ge incorporation can be attributed to the presence of Si−O−Ge and Ge−O−Ge into the zeolite structure. These results are in good agreement with the expansion of unit cell volume and they are consistent with the isomorphic substitution of Ge into the ITQ-7 framework. However, the above techniques do not give any evidence on the location of Ge atoms, and it cannot be established if they are randomly distributed or, on the contrary, preferentially occupy some T sites. Since the theoretical calculations shown above indicate that the incorporation of Ge in the most stressed positions located at the D4MR units is

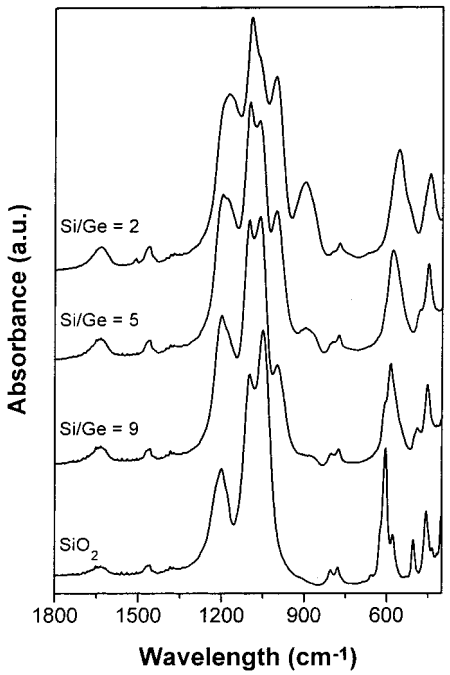

Figure 6. Infrared spectra of as-made pure silica and Ge-ITQ-7 samples, the germanium content increases from top to bottom.

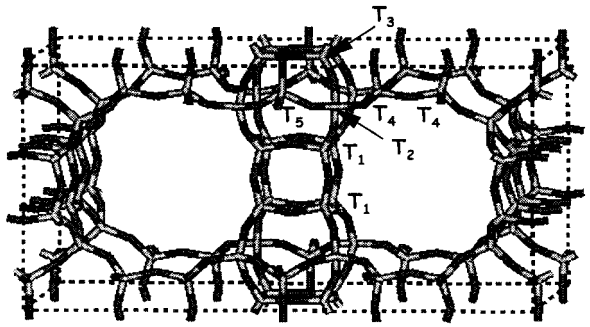

Figure 7. Crystal structure of ITQ-7 (ISV), where the crystallographic sites are marked.

TABLE 4: Crystallographic Sites, Multiplicity, and Connectivity in Zeolite ITQ-7[7]

site	multiplicity	connectivity
T1	16	3T1, 1T2
T2	16	1T1, 1T3, 1T4, 1T5
T3	8	2T2, 2T3
T4	16	3T4, 1T2
T5	8	2T2, 2T5

energetically favored, we have carried out multinuclear MAS NMR studies in order to investigate the location of Ge atoms within the different T positions in the ITQ-7 structure.

Solid-State NMR of Si,Ge-ITQ-7. The ISV topology possesses a three-dimensional system of 12MR channels, and has the peculiarity of presenting double four-membered rings cages (D4MR). The Rietveld refinement of the XRD pattern of calcined ITQ-7 as tetragonal in the topological symmetry $P4_2/mmc$ led to the model presented in Figure 7 with five crystallographic tetrahedral sites, and two structurally different D4MRs cages, one of them formed by eight T1 sites and the another one by eight T4 tetrahedra.[7] The site multiplicity and connectivity of this structure is depicted in Table 4.

The ^{19}F MAS NMR spectrum of sample Si-ITQ-7, displayed in Figure 8 (Si/Ge = ∞), is formed by an asymmetric peak at −38 ppm typical of fluorine into D4MRs cages. The presence of a low field shoulder becomes evident when the spectrum is

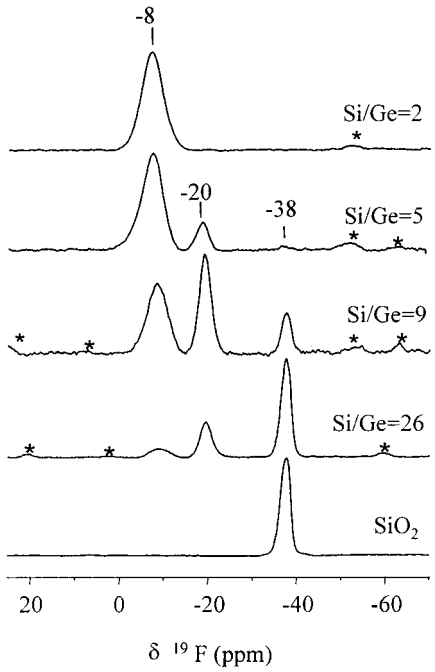

Figure 8. ^{19}F MAS NMR spectra of pure silica and germanium-containing ITQ-7 samples, the germanium content increases from bottom to top.

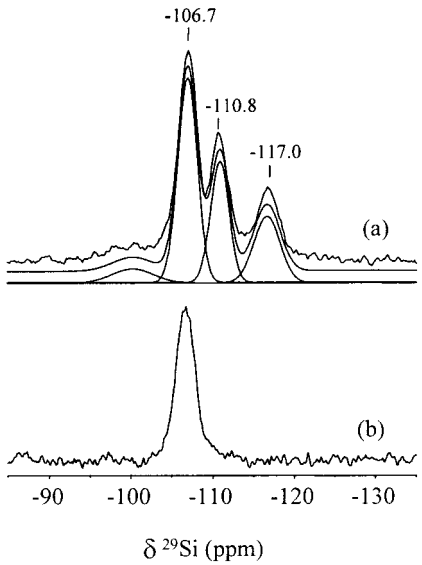

Figure 9. (a) ^{29}Si Bloch decay, and (b) ^{19}F to ^{29}Si cross polarization MAS NMR spectra of pure silica ITQ-7.

expanded, which according to previous publications[7] agrees with the location of the fluoride ions within two structurally different D4MR subunits.[7] As is shown in Figure 8, small amounts of Ge in the ITQ-7 (Si/Ge = 26) produces the appearance of two new resonances at −20 ppm and at ca. −8 ppm. The relative intensity of both peaks, specially that at −8 ppm, grows at the expense of the signal at −38 ppm as the Ge content in the zeolite increases (Figure 8), pointing out the incorporation of Ge into the coordination shell of fluorine. Indeed, the chemical shift of ^{19}F atoms within D4MRs in cloverite has been reported to depend on the chemical composition of the cage.[22] Thus, the spectra of Figure 8 strongly suggest that Ge substitutes for Si atoms into the D4MR units, and that the three peaks are originated by fluorine into D4MR cages of three different compositions. The resonance at −38 ppm is assigned to F (8Si),

TABLE 5: ^{29}Si Chemical Shifts and Relative Populations of the Different Components Derived from the Simulation of the ^{29}Si MAS NMR Spectra of the ITQ-7 Zeolites Samples

		A		B		C		Si−O$^-$ and Si (*n* Ge)[c]			Si (*n* Ge)[c]
sample	*N* Ge/100[a]	δ ^{29}Si	N/100[b]	δ ^{29}Si	N/100[b]	δ ^{29}Si	N/100[b]	δ ^{29}Si	δ ^{29}Si	δ ^{29}Si	δ ^{29}Si
Si-ITQ-7	0	−106.6	47	−110.8	25	−117.0	21			−99.3(7)	
26Ge-ITQ-7	4	−106.8	34	−110.6	22	−117.1	22			−99.1(7)	−102.9(11)
9Ge−ITQ-7	9	−107.2	25	−111.1	18	−117.1	21			−99.0(9)	−103.3(18)
5Ge-ITQ-7	17	−108.2	19	−111.2	10	−117.3	20		−96.1(5)	−99.7(7)	−104.0(22)
2Ge-ITQ-7	33	−108.8	14	−112.5	5	−117.2	15	−93.5(2)	−97.1(3)	−100.4(10)	−104.8(18)

[a] Number of Ge atoms over 100 tetrahedral (Si+Ge) atoms derived from chemical analysis. [b] Si population expressed in number of atoms per 100 tetrahedral (Si+Ge) deduced from chemical analysis and ^{29}Si MAS NMR spectra (see text). [c] The number in parentheses is the signal intensity, expressed in atoms of Si per 100 tetrahedral (Si+Ge) atoms.

and the peaks at −20 and −8 ppm to F ((8 − n_1)Si, n_1Ge) and to F ((8 − n_2)Si, n_2Ge), respectively, being $n_2 > n_1$.

Figure 9 compares the ^{29}Si Bloch decay (BD) and the ^{19}F to ^{29}Si CP MAS NMR spectra of pure silica ITQ-7 (sample Si-ITQ-7). The BD spectrum consists of three peaks at −106.7 ppm (peak A), −110.8 (peak B), and at −117.0 ppm (peak C) of Si (4 Si) units in nonequivalent crystallographic positions, and a low field component at −100 ppm due to defect sites of SiOH and/or SiO$^-$ type. The application of the ^{19}F to ^{29}Si cross polarization technique to zeolite Si-ITQ-7 selectively enhances the signal at −106.7 ppm, being the only one appearing in the spectrum of Figure 9b. In this experiment, the nuclear magnetization of fluorine must be transferred to silicon atoms and this is only possible if the two types of nucleus are close, which allows the attribution of the resonance A at 106.7 ppm to Si (4 Si) atoms in the D4MRs units. This assignment is further supported by the intensity of this peak; this accounts for 50% of the total ^{29}Si BD signal, which coincides with population of the sites involved in the formation of D4MR units in the ITQ-7 topology (see Figure 7 and Table 4).

Figure 10 shows the ^{29}Si BD spectra of zeolite ITQ-7 with different Ge content and the results of the decomposition using individual lines. At first sight, it is evident that the incorporation of Ge is accompanied by a decrease in the intensity of signal A at ca. −107 ppm, and an increase of the low field region of the spectra. The appearance of new low field signals has been previously reported for Ge containing ZSM-5, and attributed to Si((4 − *n*)Si, *n*Ge) environments[19,23] generated by the incorporation of Ge into the zeolite framework. Therefore, the evolution of the ^{29}Si MAS NMR spectra with increasing the Ge content (see Figure 10) supports the substitution of Ge for Si in the ITQ-7 structure.

The results obtained by decomposition of the ^{29}Si MAS NMR spectra are summarized in Table 5. To analyze the results quantitatively, the area of the ^{29}Si spectra of the ITQ-7 samples has been varied to reflect the chemical composition of the samples. Accordingly, the ^{29}Si BD spectrum has been normalized to 100 Si atoms for zeolite Si-ITQ-7, and progressively decreased to 67 Si atoms for zeolite 2Ge-ITQ-7, which contains 33 Ge atoms over 100 T atoms. Therefore, the intensity of each component in the ^{29}Si spectra is referred in Table 5 as the number of Si atoms per 100 T atoms, in which T accounts for both Si and Ge.

Before the analysis of Table 5, we shall consider the modification of the ^{29}Si NMR by the incorporation of Ge. The substitution of one Si atom at a crystallographic site T_s by one Ge atom will produce (i) a decrease of the Si(4Si) peak of sites T_s, and (ii) the incorporation of one Ge atom into the second coordination shell of silicon atoms at adjacent sites T_y. As a consequence, also the Si(4Si) peak intensity of sites T_y will decrease, which will be accompanied by the appearance of a new low field signal of Si(3Si, 1Ge) (at T_y positions). The results

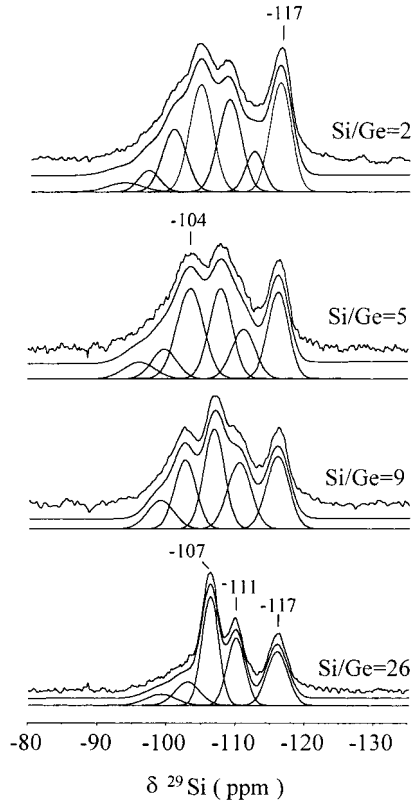

Figure 10. ^{29}Si Bloch decay MAS NMR spectra of Ge-ITQ-7 samples, the germanium content increases from bottom to top.

summarized in Table 5 show that the progressive incorporation of Ge into the ITQ-7 structure provokes a decrease of signals A and B, whereas signal C remains practically constant except for zeolite 2Ge-ITQ-7 with the highest Ge content. Therefore, at contents below 33% of T atoms, Ge does not substitute for Si atoms of type C resonating at −117 ppm and for Si atoms at framework sites adjacent to C positions. This result proves that Ge is not randomly distributed in the ITQ-7 zeolite framework at least up to a content of 33% of Ge T atoms.

The ^{19}F NMR results indicate that Ge occupies tetrahedral sites of the D4MRs units. The incorporation of one Ge to the cage will generate four Si (3Si, 1Ge) sites, three of them at D4MR positions and the fourth at the site interconnecting the cages (T2 in the structure of the calcined zeolite; see Figure 7 and Table 4). This will produce a diminution of the signals of Si(4Si) at the D4MRs (peak A) and at the interconnecting sites, proportional to four and one silicon atoms, respectively. At the same time, a new signal corresponding to D4MR Si(3Si, 1Ge) units will appear at chemical shifts above −107 ppm. The inspection of Table 5 and Figure 10 shows that as the Ge concentration increases, signal A decreases and a new resonance at ca. −103 ppm, which can be attributed to Si(3Si, 1Ge)

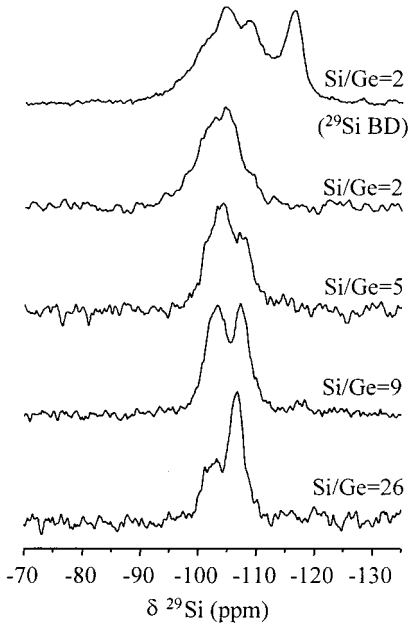

Figure 11. ^{19}F to ^{29}Si cross polarization MAS NMR spectra of Ge-ITQ-7 samples, the germanium content increases from bottom to top. For comparison, the ^{29}Si Bloch decay spectrum of zeolite ITQ-7 with a Si/Ge ratio of 2 is also included.

D4MRs atoms, increases. This assignment is further supported by the ^{19}F to ^{29}Si CP spectra shown in Figure 11, which show an enhancement of the signal at −103 ppm indicating that the corresponding silicon atoms are in the D4MRs sites. Moreover, the relative contribution of the latter peak in the CP spectra increases with the zeolite Ge content. The high-frequency region of the ^{29}Si BD NMR spectra (above −104 ppm) has been simulated using the minimum number of peaks as shown in Figure 10 and Table 4. We believe that the NMR signal in this part results from the overlapping of peaks due to Si((4 − *n*)Si, *n*Ge) and Si−OH defect groups (−100 ppm). However, the high-frequency region of the spectra is not analyzed in detailed since the poor definition of the contributing peaks leads to unreliable results.

According to the described mechanism, the substitution of a D4MR Si atom by a Ge will also decrease the intensity of the Si(4Si) peak of the crystallographic sites interconnecting the small cages (sites T2 in the structure of the calcined material schematized in Figure 7) to lower extension than signal A. This agrees with the progressive decrease of the Si(4Si) signal B (at ca. −111 ppm) when Ge atoms are incorporated to the ITQ-7 framework (see Figure 10 and Table 5). Thus, signal B must be generated, at least in part, by the Si(4Si) atoms interconnecting the small D4MRs. Simultaneously, a Si(3Si, 1Ge) must be formed in these sites, whose resonance will probably overlap with signal A. Therefore, the ^{29}Si MAS NMR results depicted in Figure 10 and Table 5 can be explained, except for sample 2Ge-ITQ-7, by the substitution of Ge for Si at the 4DMRs units exclusively. Considering calcined ITQ-7 topology (see Figure 7) and the site multiplicity and connectivity depicted in Table 4, it could be speculated for pure silica ITQ-7 that peak B is originated by T sites bridging the D4MRs cages, and peak C by the T atoms nonlinked to the D4MRs cages.

Let us analyze the ^{19}F MAS NMR spectra with the hypothesis that Ge is only located at T sites of D4MR cages. As we have discussed, the three peaks at ca. −38 ppm, −20, and −8 ppm must be originated by fluorine into D4MR cages of different composition: F(8Si), F((8 − n_1)Si, n_1Ge) and F((8 − n_2)Si, n_2Ge), respectively, with $n_2 > n_1$.

Using an approach similar to that applied to calculate the Si/Al and P/Mg ratios in zeolites[24,25] and Mg-substituted aluminophosphates,[26] respectively, the mean Si/Ge ratio in the cages will be given by the following expression:

$$\left(\frac{\mathrm{Si}}{\mathrm{Ge}}\right)_{\mathrm{cages}} = \frac{\sum_{n=0}^{n=8}(8-n)\mathrm{A}_{\mathrm{F}(n\mathrm{Ge})}}{\sum_{n=0}^{n=8} n\mathrm{A}_{\mathrm{F}(n\mathrm{Ge})}} \qquad (3)$$

where n is the number of Ge atoms in the D4MR and $A_{\mathrm{F}(n\mathrm{Ge})}$ is the area of the ^{19}F resonance of a F ((8 − n)Si, nGe) cage. If Ge is located at the D4MR units only, the Si/Ge ratio in the ITQ-7 structure can be calculated as:

$$\left(\frac{\mathrm{Si}}{\mathrm{Ge}}\right)_{\mathrm{total}} = \frac{2\sum_{n=0}^{n=8}(8-n)\mathrm{A}_{\mathrm{F}(n\mathrm{Ge})}}{\sum_{n=0}^{n=8} n\mathrm{A}_{\mathrm{F}(n\mathrm{Ge})}} + 1 \qquad (4)$$

With this hypothesis for zeolites 26Ge-ITQ-7, 9Ge-ITQ-7, and 5Ge-ITQ-7, eq 4 can be used to calculate the composition of the D4MR cages generating the ^{19}F resonances at −20 and −8 ppm, i.e., n_1 and n_2, respectively, which will help to check the consistency of our model. Since the Si/Ge ratios are known by chemical analysis, we have a system with three equations and two unknown quantities. Their solutions lead to the values of n_1 (for the resonance at −20 ppm): 1.2, 0.6, and 1.0; and of n_2 (for the resonance at −8 ppm): 2.4, 3.0, and 2.9, which are in fairly good agreement, suggesting that the Ge atoms must be at D4MR sites predominantly. Considering sample 2Ge-ITQ-7, where Ge is at D4MRs and other crystallographic sites, we obtain $n_2 \approx 5$. However, the Ge content in zeolites 26Ge-ITQ-7, 9Ge-ITQ-7, and 5Ge-ITQ-7 is insufficient to explain their ^{19}F NMR spectra if the resonance at −8 ppm is due to F (3Si, 5Ge). This proves that when the Ge population at T sites out of the D4MRs is high, the application of eq 4 leads to inconsistent results.

Therefore, assuming that Ge only occupies D4MRs positions in samples with Si/Ge ratios above 2, the ^{19}F resonances at −20 ppm and −8 ppm are assigned to fluoride ions in D4MR cages of composition (7Si, 1Ge) and (5Si, 3Ge), respectively. If this hypothesis is wrong and not all Ge atoms are at the D4MR, the peak at −8 ppm could tentatively be assigned to F (6Si, 2Ge) environments. The relative population of Ge at D4MRs and other crystallographic sites calculated with this latter attribution, and the comparison of the Si/Ge ratio calculated with the two possible assignments for the ^{19}F resonance at −8 ppm are summarized in Table 6. Even the lower field ^{19}F NMR signal is attributed to F (6Si, 2Ge), Ge shows a clear preference to substitute for Si in the D4MR, up to a certain composition. With this substitution model, a higher modification of the high field components in the ^{29}Si BD spectra (related to non-D4MR crystallographic sites) would be expected. Then, we believe that the site occupancy of Ge out of the cages for samples 26Ge-ITQ-7, 9Ge-ITQ-7 and 5Ge-ITQ-7 will probably be lower than that indicated in Table 6.

The ^{19}F NMR results suggest that not any composition of the D4MR cages is favored in the ITQ-7 framework, and D4MR units with 1 and 2 or 3 Ge atoms are formed. When the Ge content is higher than that required to have all cages with 2 or

TABLE 6: Comparison of the Si/Ge Ratios in Ge-ITQ-7 Zeolites Obtained from Chemical Analysis $(Si/Ge)_{anal}$ and Those Derived from Equation 4 in the Text[a]

sample	$(Si/Ge)_{anal}$	$(Si/Ge)_{3,1}$	$(Si/Ge)_{2,1}$	*N* Ge (D4MR)	*N* Ge
26Ge-ITQ-7	26	26.1	31.9	3.2	0.8
9Ge-ITQ-7	9	7.8	11.1	7.5	1.5
5Ge-ITQ-7	5	4.9	7.5	11.8	5.2
2Ge-ITQ-7	2	4.3	7.0	12.5	20.5

[a] The ^{19}F signal at ca. −20 ppm is attributed to F(5Si, 1Ge) in D4MR cages. The signal at ca. −8 ppm was assigned to F(5Si, 3Ge) and F(6Si, 2Ge) to calculate the $(Si/Ge)_{3,1}$ and $(Si/Ge)_{2,1}$ ratios, respectively. The number of Ge atoms, referred to 100 (Ge+Si) atoms, at double four-membered ring sites (*N* Ge D4MR), and at other crystallographic sites (*N* Ge), have been deduced from the $(Si/Ge)_{2,1}$ and $(Si/Ge)_{anal}$ ratios.

3 atoms (^{19}F peak at −8 ppm) the occupancy of crystallographic sites which are not located at the D4MR will increase. Indeed, this is the case for sample 2Ge-ITQ-7; all the ^{29}Si NMR peaks are modified by the presence of Ge, indicating a site population different to that occurring at lower Ge contents. The data reported in Table 6, assuming a composition of (6Si, 2Ge) for D4MR cages richer in Ge, indicate a drastic increase in Ge in the population of crystallographic sites out of the D4MR for 2Ge-ITQ-7 sample.

To summarize, the analysis of ^{19}F and ^{29}Si NMR spectra of Si- and Si,Ge-ITQ-7 zeolites gives evidence that Ge atoms are not randomly distributed in the nonequivalent crystallographic sites, but preferential occupancy occurs. Above a Si/Ge ratio of 2, Si(4Si) sites giving signal C plus those linked to them, accounting for a population above 20% of T crystallographic positions, are not occupied. For these samples, our results are consistent with the incorporation of Ge atoms to the D4MR only, although we cannot completely rule out a certain low occupancy of other sites. In any case, our results suggest that a maximum of two or three Ge atoms in the D4MR units are accommodated in the structure of ITQ-7. When all cages reach this composition, Ge atoms occupy other positions, including sites C and/or those linked to them.

The fact that apparently no more than 3 Ge atoms are actually incorporated in the D4MR units of ITQ-7 can be also interpreted in terms of the theoretical results documented in Tables 1 and 2. It is worth noting that, though the stability of the cluster models increases almost linearly with the Ge content, the optimized geometrical parameters indicate that the occurrence of more than 2 Ge atoms in the unit brings about significant structural distortions. In the actual zeolitic frameworks the D4MR unit is not as free to relax as in the isolated cluster considered in the calculations, due to the structural constraints imposed by the rest of the structure. Such constraints are not easy to be simulated at the ab initio level considered in the present work, but, in principle, large distortions of the D4MR unit with respect to the perfect crystal structure are expected to decrease the overall stability of the zeolite.

Therefore, the crystallization of the Si,Ge-ITQ-7 is to be controlled by two opposite effects, i.e., the internal stabilization of the cage due to the presence of Ge atoms and the overall structural destabilization produced by the geometric distortions. It is likely that at low Ge content the first effect is dominant, while when more than 3 Ge atoms are incorporated in the D4MR units, the second effect outweighs the internal stabilization of the cage and crystallization turns to be strongly unfavored.

We have seen that the introduction of Ge in D4MR positions accelerates the nucleation of Si-Ge ITQ-7. In the case of the ITQ-7 pure silica polymorph synthesis, it has been reported that the introduction of Al in the synthesis gel avoids the crystallization of the zeolite.[27] However, the ITQ-7 structure can be synthesized in the presence of B,[28] and samples with a Si/B framework ratio ≥ 30 have been prepared. We have found that when introducing Ge in the synthesis gel (Si/Ge = 5 and Si/Ge =10), the presence of Al (Si/Al = 50) does not stop the synthesis of ITQ-7 and the crystallization proceeds successfully in less than 12 h incorporating Al into the framework as demonstrated by the ^{27}Al MAS NMR analysis (spectrum not shown) (Si+Ge/Al = 110). The resultant Si,Ge,Al-ITQ-7 samples have also been analyzed by ^{29}Si and ^{19}F MAS NMR and it is found that Ge selectively occupies T positions in the D4MR.

In an analogous way, when Ti is incorporated in the gel (Si+Ge/Ti = 50) the presence of Ge allows also the synthesis of Ti-ITQ-7 in less than 12 h,[29] and again ^{29}Si and ^{19}F MAS NMR spectra show that Ge occupies selectively T positions in the D4MR of the Ti-ITQ-7 sample.

In conclusion, we have found by theoretical calculations that Ge incorporation in a D4MR cluster increases its stability. Thus, when Ge was introduced in the synthesis gel, the crystallization rate of ITQ-7 zeolite, which contains D4MR in its structure, strongly increases. Ge incorporation in framework positions has been proved by observing the unit cell volume expansion toward the Ge content. Moreover, it has been concluded from ^{29}Si and ^{19}F MAS NMR results that Ge preferentially occupies T positions at the D4MR cages. Therefore, we conclude that the introduction of Ge in the D4MR of ITQ-7 zeolite may facilitate the synthesis of this material, due to the stabilization of the structure. This could be a more general effect and, in this way, the introduction of Ge could accelerate the synthesis of pure silica zeolites with D4MR in their structure.

Acknowledgment. We thank the Spanish CICYT for financial support (Project MAT97-1016-C02-01). We thank Dr. Sastre for helpful discussions and simulations of the XRD patterns.

References and Notes

(1) Lobo, R. F.; Zones, S. I.; Davis, M. E. *J. Inclusion Phenom. Mol. Recognit. Chem.* **1995**, *21*, 47.

(2) Nakagawa, Y.; Zones, S. I. *Synthesis of Microporous Materials*; Occelli, M. L., Robson, H., Eds.; Van Nostrand Reinhold: New York, 1992; Vol. 1, p 222; Nakagawa, Y.; Zones, S. I. WO 96/29285, 1996; Zones, S. I.; Olmstead, M. M.; Santilli, M. M. *J. Am. Chem. Soc.* **1992**, *114*, 4195.

(3) Gies, M.; Marler, B. *Zeolites* **1992**, *12*, 42.

(4) Lewis, D. W.; Willock, D. I.; Catlow, C. R. A.; Thomas, J. M.; Hutchings, G. I. *Nature* **1996**, *382*, 604.

(5) Geisinger, K. L.; Gibbs, G. V.; Navrotsky, A. *Phys. Chem. Miner.* **1985**, *11*, 66.

(6) Helmkamp, M. M.; Davis, M. E. *Annu. Rev. Mater. Sci.* **1995**, *25*, 161.

(7) Villaescusa, L. A.; Barret, P. A.; Camblor, M. A. *Angew. Chem., Int. Ed.* **1999**, *38*, 1997.

(8) Piccione, P. M.; Laberty, Ch.; Yang, S.; Camblor, M. A.; Navrotsky, A.; Davis, M. E. *J. Phys. Chem. B* **2000**, *104*, 10001.

(9) O'Keefe, M.; Yaghi, O. M. *Chem. Eur. J.* **1999**, *5*, 2796.

(10) Li, H.; Yaghi, O. M. *J. Am. Chem. Soc.* **1998**, *120*, 10569.

(11) Zicovich-Wilson, C. M.; Corma, A. *J. Phys. Chem. B* **2000**, *104*, 4134.

(12) Guth, J. L.; Wey, R. *Bull. Soc. Fr. Minéral. Crystallogr.* **1989**, *92*, 105.

(13) Frisch, M. J.; Trucks, G. W.; Schlegel, H. B.; Gill, P. M. W.; Johnson, B. G.; Robb, M. A.; Cheeseman, J. R.; Keith, T.; Petersson, G. A.; Montgomery, J. A.; Raghavachari, K.; Al-Laham, M. A.; Zakzewski, V. G.; Ortiz, J. V.; Foresman, J. B.; Cioslowski, J.; Stefanov, B. B.; Nanayakkara, A.; Challacombe, M.; Peng, C. Y.; Ayala, P. Y.; Chen, W.; Wong, M. W.; Andres, J. L.; Replogle, E. S.; Gomperts, R.; Martin, R. L.; Fox, D. J.; Binkley, J. S.; Defrees, D. J.; Baker, J.; Stewart, J. P.; Head-Gordon, M.; Gonzalez, C.; Pople, J. A. *Gaussian 94*, Revision E.1; Gaussian, Inc.: Pittsburgh, PA, 1995.

(14) Saunders, V. R.; Dovesi, R.; Roetti, C.; Causà, M.; Harrison, N. M.; Orlando, R.; Zicovich-Wilson, C. M. *CRYSTAL98 User's Manual*; Università di Torino: Turin, 1999.

(15) Ugliengo, P.; Civalleri, B.; Dovesi, R.; Zicovich-Wilson, C. M. *Phys. Chem. Chem. Phys.* **1999**, *1*, 545.

(16) Guth, J. L.; Kessler, H.; Wey, R. *Stud. Surf. Sci. Catal.* **1986**, *28*, 121.

(17) Camblor, M. A.; Corma, A.; Valencia, S. *Chem. Commun.* **1996**, 2365. Koller, H.; Wölker, A.; Villaescusa, L. A.; Díaz-Cabañas, M. J.; Valencia, S.; Camblor, M. A. *J. Am. Chem. Soc.* **1999**, *121*, 3368.

(18) Guth, J. L.; Caullet, P.; Seive, A.; Patarin, J.; Delprato F. *Guidelines in Mastering the Properties of Molecular Sieves*; Plenum Press: New York, 1990; p 69. Guth, J. L.; Kessler, H.; Higel, J. M.; Lamblin, J. M.; Patarín, J.; Seive, A.; Chezeau, J. M.; Wey, R. *ACS Symp. Ser.* **1998**, *398*, 176.

(19) Kosslick, H.; Tuan, V. A.; Fricke, R.; Peuker, Ch.; Pilz, W.; Storek, W. *J. Phys. Chem.* **1993**, *97*, 5678.

(20) Blasco, T.; Lestrat, V.; Rey, F.; Vidal J. A. To be published.

(21) Lazarev, A. N.; Mirgorodsky, A. P.; Ignat′ev, I. S. K*olebatelnye Spektry Sloshnych Okislov (Russ)*; Nauka: Leningrad, 1975.

(22) Schott-Darie, C.; Delmotte, L.; Kessler, H.; Benazzi, E. *Solid State Nucl. Magn. Reson.* **1994**, *3*, 43.

(23) Gabelica, Z.; Guth, J. L. *Stud. Surf. Sci. Catal.* **1989**, *49a*, 421.

(24) (a) Engelhardt, G.; Lohse, U.; Lipmaa, E.; Tarmak, M.; Mägi, M. Z. *Anorg. Allg. Chem.* **1981**, *482*, 49. (b) Thomas, J. M.; Fyfe, C. A.; Ramdas, S.; Klinowski, J.; Gobbi, G. C. *J. Phys. Chem.* **1982**, *86*, 3061.

(25) Thomas, J. M.; Fyfe, C. A.; Randas, S.; Klinowski, J.; Gobbi, G. C. *J. Phys. Chem.* **1982**, *86*, 3061.

(26) Barri, P. J.; Klinowski, J. *J. Phys. Chem.* **1989**, *93*, 5972.

(27) Villaescusa, L. A. Ph.D. Thesis, Universidad Politécnica de Valencia, Spain, 1999.

(28) Corma, A.; Díaz-Cabañas, M. J.; Fornés, V. *Angew. Chem., Int. Ed.* **2000**, *39*, 2346.

(29) Corma, A.; Díaz-Cabañas, M. J.; Domine, M. E.; Rey, F. *Chem. Commun.* **2000**, *18*, 1725.